Carbon Vol. 24, No. 5, pp. 639–647, 1986
Printed in Great Britain.

0008–6223/86 $3.00 + .00

ELECTROMECHANICAL BEHAVIOR OF GRAPHITE INTERCALATED WITH BROMINE

D. D. L. CHUNG and LAN W. WONG
Department of Metallurgical Engineering and Materials Science, Carnegie-Mellon University, Pittsburgh, PA 15213, U.S.A.

(*Received* 10 *October* 1985; *in revised form* 3 *March* 1986)

Abstract—Graphite–bromine was found to produce a tensile stress (up to about 3 MPa) along the *c*-axis upon heating by the passage of an electric current (with a current density of up to about 5×10^5 A/m^2) along the *c*-axis. This electromechanical effect was reversible and allowed electromechanical switching. The stress increase started at about 100°C upon heating. The *c*-axis electrical resistivity of graphite–bromine was found to increase and then decrease upon heating and to increase and then decrease upon subsequent cooling, when the graphite–bromine sample was under mechanical constraint from expansion along the *c*-axis. These effects are attributed to the initiation of intercalate bubble formation as the sample was heated.

Key Words—Intercalation, bromine, electrochemical behavior, bubble formation.

1. INTRODUCTION

During the past ten years, there has been a tremendous growth in studying the structure and properties of graphite intercalation compounds. Because of the low electrical resistivity of graphite intercalation compounds, much work has been done to understand the electrical behavior of these materials. However, no attention has previously been given to the electromechanical behavior. This paper provides the first observation of an electromechanical effect in graphite intercalation compounds. The observation was made in graphite–bromine. In this phenomenon, the intercalation compound produces a tensile stress (up to about 3 MPa) along the *c*-axis upon passage of an electric current (with a current density of up to about 5×10^5 A/m^2) along the *c*-axis. The effect is reversible and promises the application of graphite intercalation compounds in electromechanical devices.

The electrical resistivity of graphite intercalation compounds has been a topic of much scientific and technological interest. The *a*-axis electrical resistivity of graphite is greatly decreased by intercalation, but the *c*-axis electrical resistivity is generally increased by intercalation[1]. Intercalation also affects the temperature dependence of the electrical resistivity, particularly the *c*-axis electrical resistivity. The *c*-axis electrical resistivity of pristine graphite decreases with increasing temperature, whereas that of intercalated graphite increases with increasing temperature[1]. This paper describes the first observation of an anomalous effect of heating on the *c*-axis electrical resistivity of intercalated graphite when the intercalated graphite is constrained from expansion along the *c*-axis.

2. EXPERIMENTAL

2.1 *Sample Preparation*

2.1.1 *Sample A (for electromechanical measurements).* Highly oriented pyrolytic graphite (HOPG), which was kindly provided by Union Carbide Corporation, was intercalated with bromine to stage 2 by exposure to bromine vapor at room temperature. Subsequently it was allowed to desorb in air at room temperature. At the time of the electromechanical data collection, desorption had occurred for about 12 hr, so that, at the start of the measurement, the intercalate concentration was about 70 wt. % bromine, and the stage was mixed (2 and 3).

The sample thickness (along the *c*-axis) was 0.058 cm. The cross section of the sample (perpendicular to the *c*-axis) was trapezoidal (nearly rectangular), with dimensions $1.036 \times 0.236 \times 0.925 \times 0.310$ cm.

Two electrical contacts were made on each of two opposite surfaces (perpendicular to the *c*-axis) of the sample by using flattened copper wires (0.014 in. diameter), which were attached to the sample by silver conducting paint. This resulted in a four-probe configuration. A contact on each surface served as a current probe, while the other contact on each surface served as a voltage probe. Current probes were used for the passage of an electric current along the *c*-axis; voltage probes were used for measuring the voltage drop across the sample along the *c*-axis.

2.1.2 *Sample B (for thermomechanical measurements).* Another HOPG sample (Sample B) was similarly intercalated with bromine to stage 2. Subsequently, it was allowed to desorb in air at room temperature. At the time of the thermomechanical data collection, desorption had occurred for about 6 hr, so that, at the start of the measurement, the intercalate concentration was about 75 wt. % bromine and the stage was mixed (2 and 3).

The sample thickness (along the *c*-axis) was 0.071 cm. The cross-sectional area of the sample was 0.3427 cm^2.

Electrical contacts were placed on Sample B in the same way as Sample A.

2.2 *Experimental Techniques*

2.2.1 *Electromechanical measurements.* The graphite–bromine sample (Sample A), which had four

probes attached to it, was placed between the steel compression plates of an Instron Model 1125 (22,000 lb. load frame) mechanical testing system with a machine stiffness of 1×10^6 lb/in operating in the compression mode. During the experiment, the cross-head of the machine was kept fixed. For a typical maximum load of 5 Kg, the strain (fractional expansion) in the sample was 0.05%. The sample was insulated from the steel plates by glass slides. A chromel–alumel thermocouple was placed beside the sample, such that it almost touched the sample (about 0.1 mm from the sample).

A 24 V, 12 A DC variable power supply was connected to the current probes, such that it was in series with a standard 1 m Ω resistor. The current was measured by measuring the voltage across the standard resistor.

Current was passed through the current probes into the sample along the *c*-axis while the cross-head of the Instron system was kept fixed and a chart recorder recorded the compressive force which the Instron system had to supply to the sample in order to counteract the tensile force which the sample produced. Simultaneously, the current through the current probes, the voltage across the voltage probes and the temperature of the thermocouple were recorded by chart recorders. The current was increased and then decreased in steps; forty cycles were carried out.

2.2.2 *Thermomechanical measurements.* The graphite–bromine sample (Sample B) was placed between the ends of two glass (Pyrex) rods. The other end of each of the glass rods had been fixed to one of the steel compression plates of the Instron mechanical testing system mentioned above. A chromel–alumel thermocouple was placed beside the sample, such that it almost touched the sample. The sample and parts of the glass rods were surrounded by a small resistance heater coil, which extended about 2.5 cm both above and below the sample. The temperature detected by the thermocouple was controlled by a TECCO temperature programmer.

In order to measure the electrical resistivity along the *c*-axis, a 24 V, 12 A DC variable power supply was connected to the current probes, such that it was in series with a standard 1 m Ω resistor. The current was measured by measuring the voltage across the standard resistor. The power used was much less than that used for Sample A because Sample A was heated by the electric power whereas Sample B was heated by the heater coil.

Sample B was heated while the cross-head of the Instron system was kept fixed and the chart recorder recorded the compressive force which the Instron system had to supply to the sample in order to counteract the tensile force which the sample produced. Simultaneously, the current through the current probes, the voltage across the voltage probes and the temperature of the thermocouple were recorded by chart recorders. The temperature was increased and then decreased in steps.

The stress contributed by the thermal expansion of the glass rods as a function of temperature during heating and cooling was measured by having no sample between the rods and allowing the rods to touch one another. It was found that the thermal expansion of the glass rods contributed a stress ranging from 0.02 MPa at 60°C to 0.19 MPa at 225°C. This correction had been made in the stress data reported here.

The thermomechanical measurement was also carried out on a pristine HOPG sample. The measured stress as a function of temperature was approximately the same as that obtained with the glass rods touching one another. This means that the thermal expansion of pristine HOPG contributed negligible stress. The *c*-axis electrical resistivity was observed to increase monotonically with temperature during heating, such that the resistivity increased by 15% at 95°C and by 78% at 224°C. Upon cooling, the resistivity decreased monotonically, though with much hysteresis.

2.3 *Experimental Results*

2.3.1 *Electromechanical measurements.* Figure 1 shows the variation of stress with electric power (product of the voltage and the current) as the power was increased and decreased during Cycle No. 2. As the power was increased, the stress started to increase when the power reached 0.3 W and the increase occurred gradually from 0 to 1.2 MPa as the power increased from 0.3 to 4 W. At 4 W, the stress increased abruptly from 1.2 to 2.2 MPa. Further increase in power from 4 to 5 W caused the stress to decrease to 1.7 MPa. Subsequently decrease of the power from 5 to 3 W caused the stress to decrease only slightly. Below 3 W, the stress decreased significantly, though gradually; a stress of zero was reached at about 0.5 W. The corresponding variation of the *c*-axis electrical resistivity with electric power is shown in Fig. 2. The resistivity first increased and then decreased as the power was increased and the same effect was observed as the power was decreased. Upon increasing the power, the steepest drop in resistivity occurred at 4 W, which is the power at which the stress abruptly increased. Upon decreasing the power, the resistivity was quite constant from 5 to 3 W; at 3 W the resistivity started to increase upon further decrease of the power. Similarly, the stress decreased only slightly when the power was decreased from 5 to 3 W; at 3 W, the stress started to decrease significantly upon further decrease of the power. Hence, the decrease in resistivity observed upon increasing the power is associated with the increase in stress and the increase in resistivity observed upon decreasing the power is associated with the decrease in stress. In Fig. 2 the maximum resistivity occurred at about 2 W, but this maximum corresponds to no distinguished feature in the variation of stress with power.

Figure 3 shows the variation of stress with power in Cycle No. 10. As the power was increased, the stress started to increase when the power reached 2 W. The increase occurred gradually from 0 to 1.5 MPa as the power was increased from 2 to 10 W. At

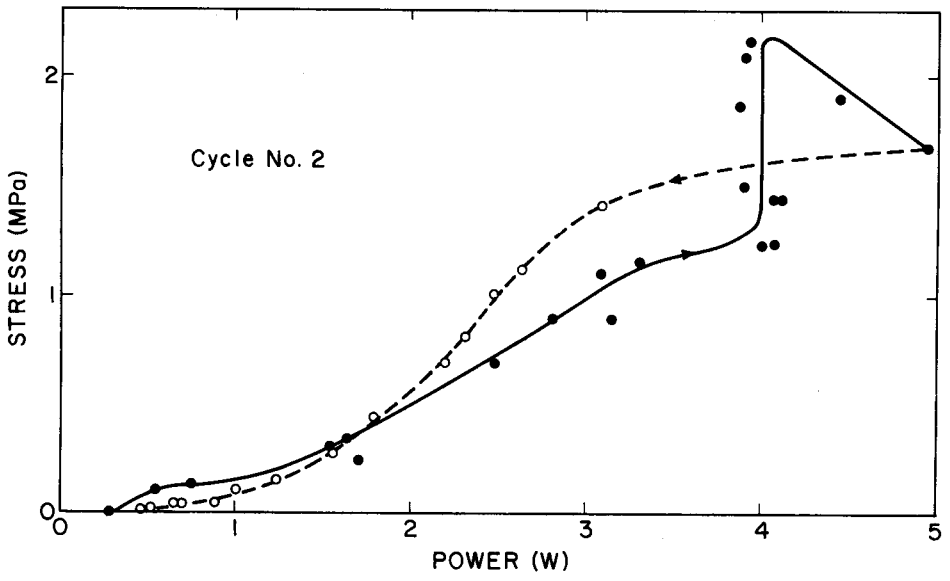

Fig. 1. Variation of stress with the electric power as the power was increased (full line and solid circles) and decreased (dashed line and open circles) during Cycle No. 2.

10 W, the stress increased abruptly from 1.5 to 2.1 MPa and did not decrease upon further increase of the power to 11.3 W. Subsequent decrease of the power caused the stress to decrease gradually to zero. Figure 4 shows the corresponding variation of the *c*-axis electrical resistivity with power as the power was increased and decreased during Cycle No. 10.

The increase and then decrease in the *c*-axis electrical resistivity upon increasing or decreasing the power were observed in all cycles. The dependence of the resistivity on the cycle number is shown in Fig. 5, where the initial resistivity of Cycle N is the same as the final resistivity of Cycle N-1. The initial resistivity at the beginning of a cycle as well as the maximum resistivity of a cycle decreased with increasing cycle number. The decrease was large in Cycles 1 and 2, but was small or zero in subsequent cycles. In particular, the maximum resistivity in Cycle 1 upon decreasing the power (cooling) was the same as the maximum resistivity in Cycle 2 upon increasing the power (heating).

The decrease of the resistivity with increasing cycle

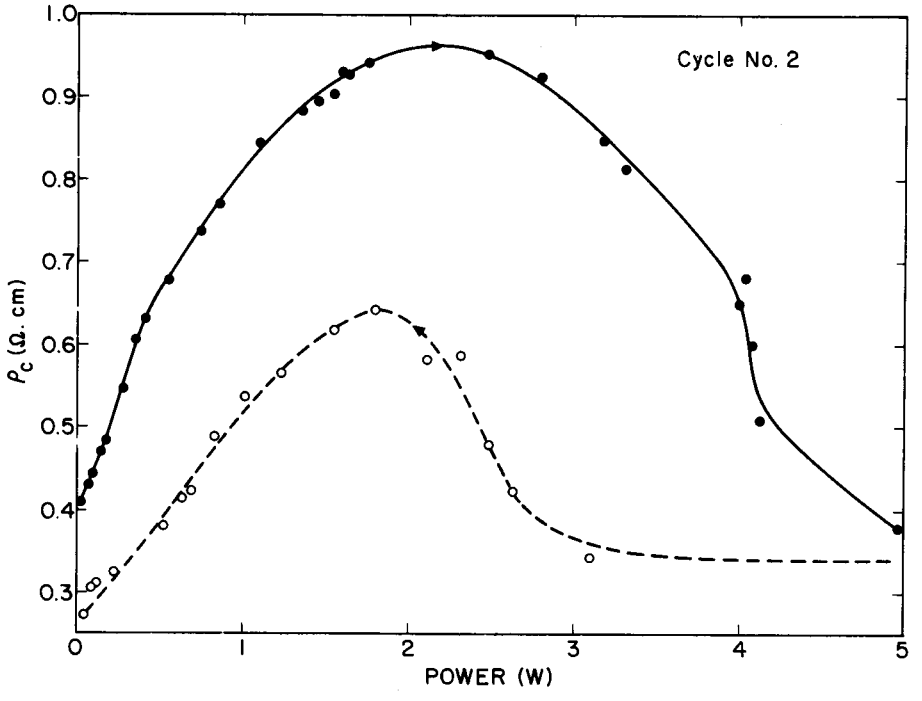

Fig. 2. Variation of the *c*-axis electrical resistivity with electric power as the power was increased (full line and solid circles) and decreased (dashed line and open circles) in Cycle No. 2.

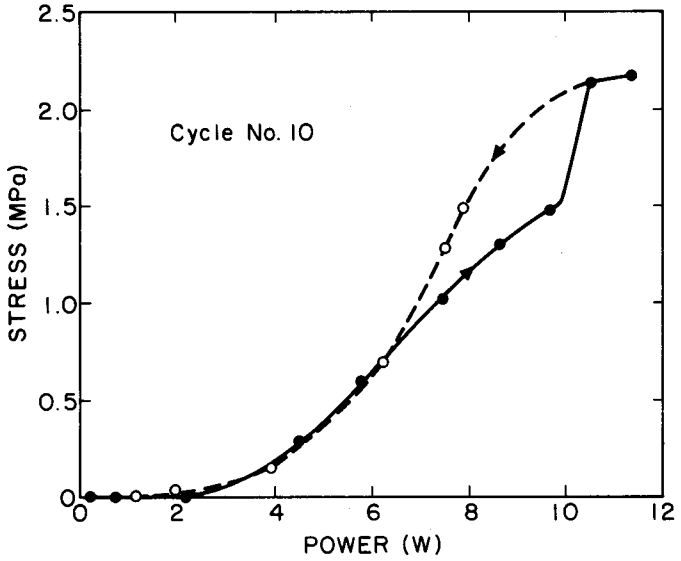

Fig. 3. Variation of stress with the electric power as the power was increased (full line and solid circles) and decreased (dashed line and open circles) during Cycle No. 10.

number (Fig. 5) is attributed to the effect of stress on the resistivity. Figure 6 shows the final electrical resistivity at the end of a cycle versus the maximum stress experienced in the cycle. The greater is the stress, the smaller is the final resistivity. This trend is expected since the compressive stress decreases the spacing between the graphite layers.

The decrease in stress which occurred when the power was increased beyond that needed for the jump in stress only occurred in the first several cycles, becoming less significant as the cycle number increased. This decrease is attributed to intercalate desorption, which was most significant in the first few cycles.

The passage of the electric current caused the sample to heat up, as confirmed by the thermocouple temperature measurement. Details of the temperature dependence were revealed by the thermomechanical measurements, which yielded a more uniform temperature distribution and a more accurate temperature measurement.

The increase in stress occurred in two steps. In the first step, the stress began increasing at a low power value (e.g. 0.3 W in Cycle No. 2 and 2 W in Cycle No. 10) and reached about 1 MPa. In the second step, the stress began increasing at a high power value (ranging from 4.0 W for Cycle No. 2 to 9.9 W for Cycle No. 10) and reached more than 2 MPa. Beyond Cycle No. 10 (up to Cycle No. 40), the powers for the stress increases did not increase further to any significant degree.

Figure 7 shows the effect of increasing the current from 0 to 12 A instantaneously holding the current at 12 A for 23 s, and then decreasing the current from 12 to 0 A instantaneously during Cycle No. 17. The instantaneous current increase caused the stress to rise from 0 to 2.28 MPa (maximum) in 9 s, and caused

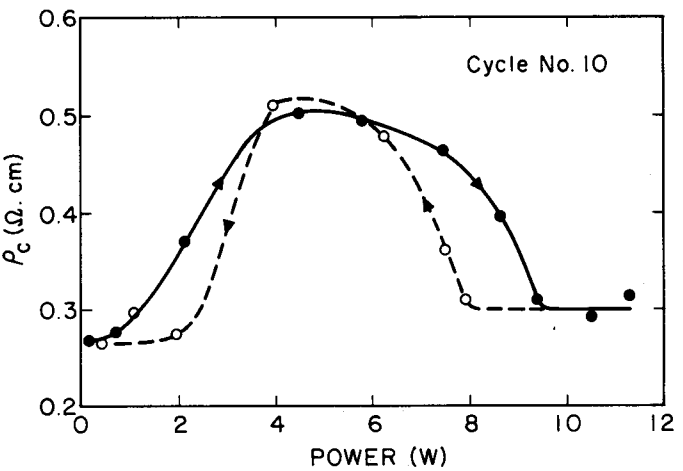

Fig. 4. Variation of the c-axis electrical resistivity with electric power as the power was increased (full line and solid circles) and decreased (dashed line and open circles) in Cycle No. 10.

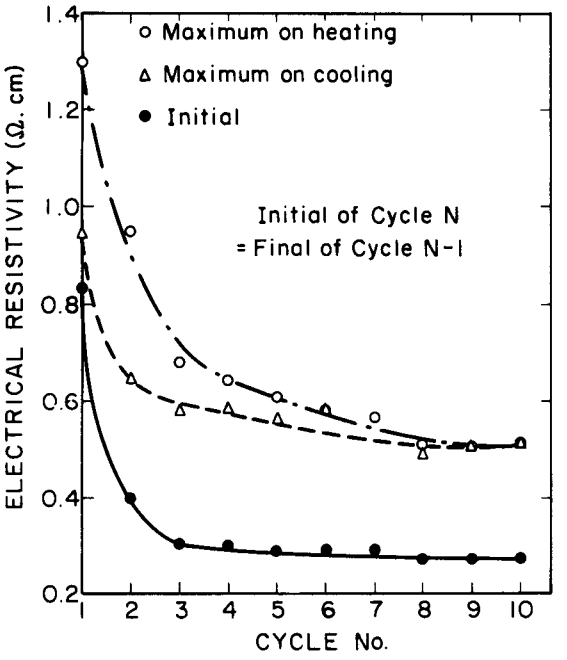

Fig. 5. The dependence of the electric resistivity on the cycle number. The maximum resistivity during heating (open circles), the maximum resistivity during cooling (open triangles) and the initial resistivity of a cycle (solid circles) are shown for each cycle.

the temperature to rise from 28 to 116°C (maximum) in 15 s. The instantaneous current decrease caused the stress to drop from 2.28 to 0.05 in 4.8 s, and caused the temperature to drop from 116 to 30°C in 25 s. Hence, although the rise and fall of the stress are closely related to those of the temperature, the rise time and fall time for the stress are considerably smaller than those for the temperature. Figure 7 also shows that the voltage increased sharply from 0 to 0.94 V in the first 0.1 s, but subsequently decayed, reaching 0.38 V at 15 s, when the temperature had reached a steady state of 116°C. Upon switching off the current at 23 s, the voltage instantaneously fell to zero. The behavior shown in Fig. 7 was observed in all cycles (Cycle No. 17–40) in which the current was instantaneously turned on (to 12 A) and off.

2.3.2 *Thermomechanical measurements.* Thermomechanical measurements were performed on Sample B. Figures 8 and 9 show the stress and *c*-axis electrical resistivity measured simultaneously as a function of temperature during stepwise heating and cooling in Cycle No. 7. The stress began to increase at about 100°C, and the increase became rapid at about 125°C. Hysteresis was observed during cooling. The electrical resistivity increased and then decreased upon heating and again increased and decreased upon subsequent cooling, such that the maximum resistivity occurred at about 125°C and the most abrupt resistivity change occurred at 100°C during both heating and cooling. The observed thermomechanical effects are consistant with the observed electromechanical effects.

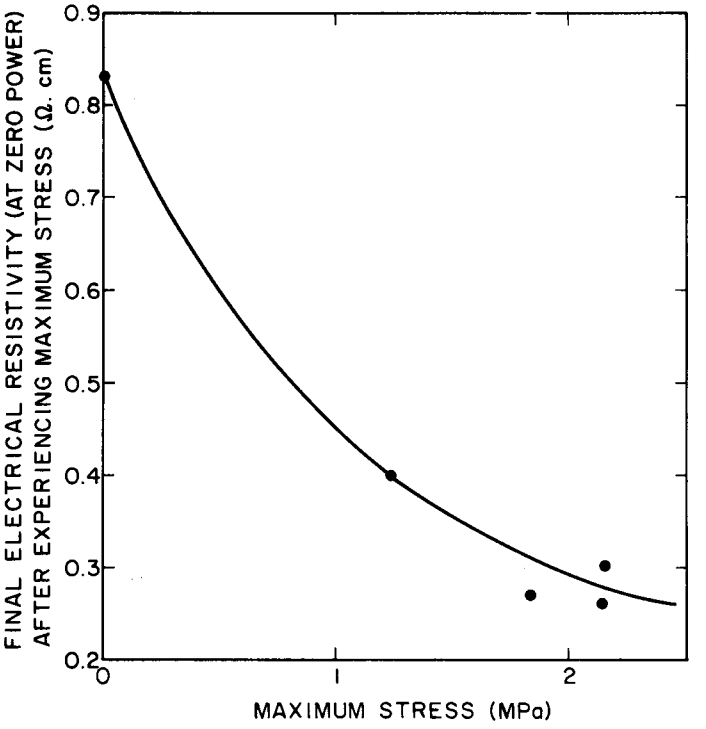

Fig. 6. The final *c*-axis electrical resistivity at the end of a cycle (i.e. at zero power) versus the maximum stress experienced in the cycle.

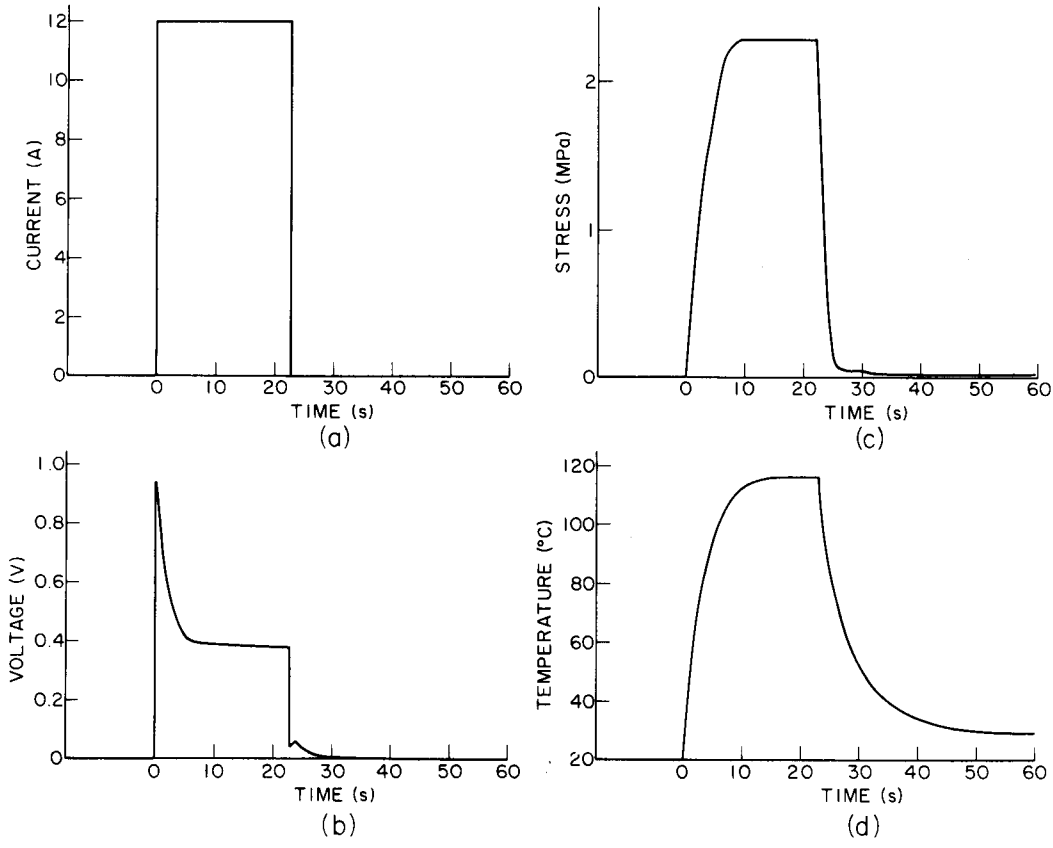

Fig. 7. The effect of current switching on the stress, temperature and voltage as a function of time in Cycle No. 17.

The changes in stress and electrical resistivity were almost completely reversible. The stress after cooling was slightly higher than that before heating (Fig. 8); the resistivity after cooling was slightly below that before heating (Fig. 9).

Similarly, thermomechanical measurements performed on pristine HOPG showed that the *c*-axis electrical resistivity of pristine HOPG increased monotonically with temperature, and that the increase was much more gradual than that in Fig. 9. Thus, the effect shown in Fig. 9, was not observed in pristine HOPG.

3. DISCUSSION

Upon the passage of current along the *c*-axis, which is the high resistivity direction, Joule heating caused the temperature of the sample to rise. The temperature rise in turn caused the sample to generate a tensile stress. It should be emphasized that the sample was constrained from expansion along the *c*-axis by the Instron load frame. The observed electromechanical or thermomechanical effect is attributed to the initiation of intercalate bubble formation. The actual expansion of the bubbles would cause exfoliation[2,3] of the intercalated graphite, but the expansion was constrained mechanically.

Figures 8 and 9 show that the abrupt increase in *c*-axis electrical resistivity at 100°C is associated with little change in the stress, whereas the decrease in the electrical resistivity at temperatures above 125°C is associated with a sharp increase in stress. This suggests that the abrupt increase in *c*-axis electrical resistivity at 100°C is associated with the formation of microcracks (or pockets) containing the intercalate and the melting of the intercalate at 100°C[4]. The decrease in resistivity and increase in stress at temperatures above 125°C are probably consequences of the change of the intercalate liquid to a compressed vapor in the graphite, which thereby underwent some bending of the graphite layers.

The fact that the resistivity after cooling was below that before heating and that the stress after cooling was higher than that before heating indicates that the bending of the graphite layers was not totally reversible, as also indicated by X-ray diffraction[2]. However, the near reversibility of the changes in stress and electrical resistivity is consistent with the fact that the three-fold twinned monoclinic in-plane intercalate structure of graphite–bromine is maintained after exfoliation on heating and collapse on subsequent cooling[2].

In a separate experiment, a pristine HOPG sample was subject to a compression test along the *c*-axis. It was found that a compressive stress of 2 MPa gave rise to a strain of -0.7% along the *c*-axis. Thus, this amount of strain might occur locally inside the graphite–bromine sample during the initiation of bubble formation.

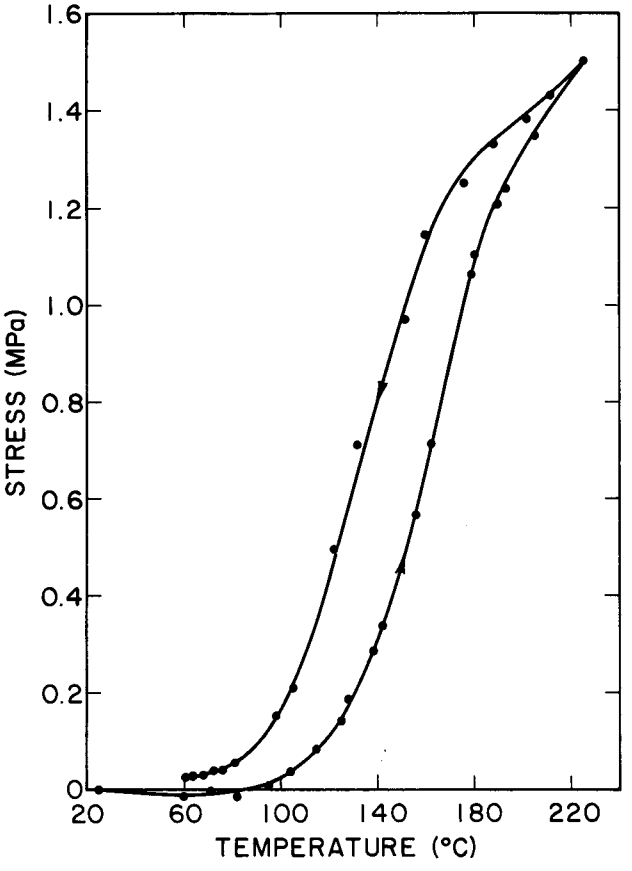

Fig. 8. Variation of stress with temperature during heating and cooling in Cycle No. 7 of the thermo-mechanical measurements.

In another separate experiment, exfoliation was allowed to occur under negligible applied mechanical constraint while electrical power (along the *c*-axis) and furnace heat were supplied to the sample. It was found that the exfoliation temperature was independent of the applied electric power. Therefore, the increase in power with cycle number is not due to the increase in the exfoliation temperature with cycle number, but may be due to the irreversible effect of the initiation of bubble formation on the electrical[5,6] and thermal behavior of the intercalated graphite.

Electrical conduction along the *c*-axis of graphite has long been an issue of controversy, but a number of defects can provide conduction paths along the *c*-axis[7]. Therefore, the electrical resistance of a sample along the *c*-axis may be modeled as that of n resistors (each of resistance R) in parallel, as illustrated schematically in Fig. 10. The total resistance R_T along the *c*-axis is given by

$$R_T = R/n.$$

The formation of microcracks (or pockets) containing the intercalate decreases n, thus increasing $1/n$. The bending of the graphite layers decreases R. The dependence of $1/n$, R and R_T ($=R/n$) on the temperature is illustrated schematically in Fig. 10. Hence, the total resistance R_T first increases then decreases.

The association of the decrease in R with the increase in stress is consistent with the report that the *c*-axis electrical resistivity of pristine graphite decreased with increasing applied pressure[8].

The anomalous temperature dependence of the *c*-axis electrical resistivity reported in this paper has not been previously observed. The closest related work is that by Miyauchi *et al.*, who observed that the *a*-axis electrical resistivity of the graphite–bromine (based on artificial graphite heat-treated at 3000°C) increased with increasing temperature (up to 800°C) and subsequently decreased with decreasing temperature under no mechanical constraint[9]. The increase in resistivity began at about 200°C upon heating; the decrease in resistivity began at about 320°C upon cooling[9]. The origin of this change in the *a*-axis resistivity is attributed to the initiation of intercalate bubble formation, which disturbs the planar nature of the graphite layers and thus increases the *a*-axis electrical resistivity. Actual exfoliation did not occur in spite of the absence of applied mechanical constraint because of the poor preferred orientation in the graphite material. The temperatures observed by Miyauchi *et al.* for change in the *a*-axis resistivity are higher than those we observed for change in the *c*-axis resistivity. The difference is due to the higher quality well-oriented graphite used in the present work, as the ease of the exfoliation increases with increasing structural perfection of the graphite material[10].

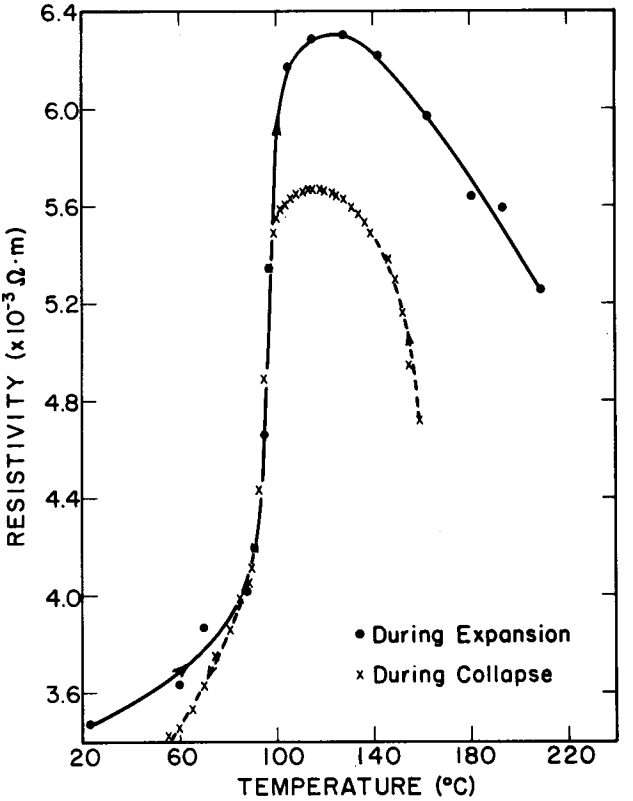

Fig. 9. Variation of the *c*-axis electrical resistivity with temperature during heating (full line and solid circles) and cooling (dashed line and crosses) in Cycle No. 7 of the thermomechanical measurements.

Without mechanical constraint, exfoliation expansion would occur and result in much larger changes in the electrical resistivity than what is reported here for the case of having mechanical constraint. The effect under no constraint is the subject of a separate publication[5]. This paper has shown that, even though exfoliation expansion can be prevented by mechanical constraint, the effect of the initiation of bubble formation on the electrical resistivity cannot be avoided. This effect must be considered in the use of intercalated graphite as an electrical conductor.

The mechanical constraint used in this work is the externally applied compression. However, similar constraints from exfoliation expansion can arise internally from the structural imperfections in the graphite material. In other words, an intercalated graphite based on a relatively poor graphite material might not be able to exfoliate, but the effect on the electrical resistivity might still be present. Based on the temperature for the collapse of the exfoliated material (i.e. the condensation of the intercalate vapor), Mazieres *et al.* suggested that, under no externally applied compression, mechanical strains equivalent to an additional pressure of about 1 atm (0.1 MPa) prevent the totally free expansion of the defects in which the bromine is trapped[6].

Since exfoliation is a phenomenon which essentially all intercalated graphite undergoes, the anomalous effect on the electrical resistivity reported here for the case of graphite–bromine is expected to apply

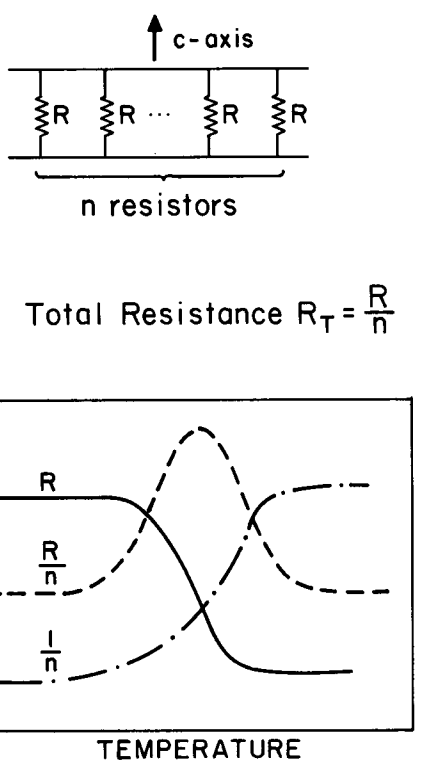

Fig. 10. Modeling the resistance of a sample along the *c*-axis as *n* resistors (each of resistance *R*) in parallel.

to many other graphite intercalation compounds as well.

Figure 7 demonstrates the capability of the intercalated graphite to serve as an electromechanical switch. The lifetime of the electromechanical switch was found to be limited by the lifetime of the contact wires, which burn out due to the heating. For copper wires used in this work (0.014 in diameter), the lifetime was 40 cycles. For copper wires of diameter 0.007 in, the lifetime was less than 1 cycle. For copper wires of diameter 0.035 in, the lifetime exceeds 58 cycles, at the end of which no sign of failure was observed. Hence, the lifetime increases with increasing diameter of the copper wires. By using thick contact wires, the lifetime is expected to be so long that practical use of the electromechanical switch is possible.

It has been reported that a compressive stress of up to 24 MPa along the *c*-axis was not sufficient to prevent the intercalation of bromine in well-oriented graphite[11]. In contrast, the stress reported in this work is the compressive stress needed to prevent the exfoliation of graphite–bromine.

Acknowledgements—Equipment support from the Materials Research Laboratory Section, Division of Materials Research, National Science Foundation, under Grant DMR 76-81561 A01 is acknowledged. Stimulating discussion with S. H. Anderson Axdal of Carnegie-Mellon University is greatly appreciated.

REFERENCES

1. A. R. Ubbelohde, *Proc. R. Soc. Lond. A.* **327,** 289 (1972).
2. S. H. Anderson and D. D. L. Chung, *Synth. Met.* **8,** 343 (1983).
3. S. H. Anderson and D. D. L. Chung, *Carbon* **22,** 253 (1984).
4. K. K. Bardhan, J. C. Wu and D. D. L. Chung, *Synth. Met.* **2,** 109 (1980).
5. D. D. L. Chung and Lan W. Wong, *Synth. Met.* **12,** 533 (1985).
6. C. Mazieres, G. Colin, J. Jegoudez and R. Setton, *Carbon* **13,** 289 (1975).
7. B. T. Kelly, *Physics of Graphite,* Applied Science Publishers, 1981, pp. 291–296.
8. L. C. F. Blackman, P. H. Dundas and A. H. Ubbelohde, *Proc. Roy. Soc. A* **255,** 293 (1960).
9. K. Miyauchi, Y. Takahashi and T. Mukaibo, *Carbon* **9,** 807 (1971).
10. W. H. Martin and J. E. Brocklehurst, *Carbon* **1,** 133 (1964).
11. G. A. Saunders, A. R. Ubbelohde and D. A. Young, *Proc. Roy. Soc. A* **271,** 512 (1963).